06500-6002-R0000

APPENDIX A

CHARACTERISTICS OF THE SOLAR WIND - MAGNETOSPHERE TRANSITION REGION

CHARACTERISTICS OF THE SOLAR WIND - MAGNETOSPHERE TRANSITION REGION

by

Frederick L. Scarf
Space Sciences Laboratory
TRW SYSTEMS
One Space Park
Redondo Beach, California 90278
(213) 679-8711, Extension 22965

The concept of a collisionless shock transition between the magnetosphere and the free streaming solar wind was originally introduced on the grounds that the interplanetary magnetic field would, somehow, bind the collisionless plasma into a conventional fluid. Details of the dissipation mechanisms were avoided, and aerodynamic analogies were used to compute the location of the shock boundary, assuming that the relevant Mach number is (u/V_A), where u is the wind speed and V_A is the Alfvén wave speed (1, 2, 3). To an amazing extent, these rough kinematical techniques do provide an accurate statistical prediction for the location of the mean proton boundary, or magnetopause, and the mean shock boundary, or position where the solar wind is first disturbed (4). However, to a large degree these predictions of the fluid or mhd model are the only ones which appear to have any detailed validity.

More rigorous studies of the magnetohydrodynamic models of the collisionless bow shock have now been carried out (5, 6, 7); and the results of these computations are available for comparison with observations.

In each case it is assumed that the collisionless plasma is completely described by the mhd equations everywhere except at the (thin) shock boundary, and the deHoffman-Teller (8) jump relations are used to evaluate the change in N, u, B, and T across the shock. The implicit assumptions contained in this approach include neglect of possible: a) charge separation electric fields associated with electron-proton mass and charge differences; b) generation of significant wave energy and momentum densities downstream from the shock; c) generation of wave modes which can travel upstream to interact with incoming particles so that the concept of a think shock discontinuity becomes invalid; d) collisionless wave-particle interactions which can accelerate particles and produce very non-Maxwellian plasma distributions.

The predictions of the fluid equations are fairly explicit. If we consider a frame of reference for which $\vec{u}$ and $\vec{B}$ are parallel, and examine the region near the nose of the shock, then for high Alfvénic Mach numbers, the deHoffman-Teller relations yield $u' \gtrsim u/4$, $N' \gtrsim 4N$, where the primed quantities refer to flow parameters just behind the shock. The predicted temperature change can be very high (e.g. $T'/T \sim 30$ for an Alfvén Mach number of 6.3) and as the flow continues on to the stagnation point, the fluid equations yield $u' \to 0$, with the residual streaming energy being converted into thermal energy.

The first particle measurements made near the stagnation point revealed the presence of hot <u>electrons</u>, rather than thermalized protons.

This was shown in early results from Explorer 12 (9) and assuming that the Cd S detector was responding to kilovolt electrons, Freeman (10) presented further evidence for the presence of very hot transition region electrons near the nose, and the VELA-2 plasma probes have recently detected electron temperatures as high as 3×10^8°K (11) beyond the magnetopause. It seems clear that the energetic electron spikes observed on IMP-1 (12, 13) and other spacecraft represent the high energy parts of hot electron distributions, and since these particles are not present in the quiescent solar wind, some fundamental collisionless acceleration mechanism must operate to produce them. Some information about this mechanism comes from the less frequent observation of similar high energy electrons upstream from the "shock"; this indicates that the acceleration may involve waves which can propagate upstream, or that collisionless acceleration is an interplanetary phenomenon associated with fast streams overtaking slow ones.

Proton measurements in the transition region reveal especially striking deviations from the predictions of the fluid model. Figure 1 shows simultaneous IMP-2 and OGO-1 interplanetary and transition region positive ion spectra (14), and it can be seen that u' far exceeds $u/4$. Moreover, although the presence of a very significant non-Maxwellian tail indicates that some protons have been accelerated, any attempt to fit a Maxwellian to this yields $T'/T << 30$. The most striking deviation from the fluid prediction is the fact that this <u>same</u> proton spectrum was simultaneously measured at widely separated points throughout the transition region by probes on VELA-3, IMP-2, and OGO-1 (14). This indicates that the shock transition is one which converts the incident wind to a new plasma state, and presumably the state is one of marginal stability with respect to some plasma instability.

Some insight into these processes is derived from examination of the wave modes associated with the free-streaming wind. Recent interplanetary measurements on Pioneer 6 (15) show that the positive ion distribution is a field-aligned bi-Maxwellian with $T_{\parallel} > T_{\perp}$. It has been demonstrated (16) that this distribution is unstable and that protons should feed energy into whistler-mode waves via the anomalous Doppler shift, with peak wave growth near the local proton gyrofrequency. Such instabilities may be especially relevant in the transition region because any disturbance induced by the proximity to the magnetosphere can drastically alter the growth rates and lead to large amplitude magnetic pulsations. Indeed extremely large amplitude, low frequency transition region disturbances have been detected with magnetometers on Pioneers 1, 5, Explorers 12, 14, OGO-1, and VELA-3. For instance, the VELA magnetometers have found quasi-sinusoidal oscillations with periods of 10 to 60 seconds and peak-to-peak amplitudes as high as 50 gamma over large segments of the transition region (17); this is very significant because the wave energy density, $(\Delta B)^2/8\pi$, is a sizeable fraction of NMU^2 so that the mhd formalism, which neglects transport of energy and momentum by waves, becomes of questionable validity.

Other plasma instabilities must certainly play a role in formation of the transition region. Figure 2 compares interplanetary, transition region (A - disturbed, B - quiet) and magnetospheric search coil power spectra at higher frequencies (18). It appears that the large transition region power density extends up to hundreds of cycles/sec, and it is possible that large amplitude magnetic pulses have caused local direction shifts so that $T_{\perp}$ exceeds $T_{\parallel}$, and the whistler mode instability at the electron gyrofrequency (19) is triggered. Possible stimulation of the electron whistler mode is of interest because for a large range of frequencies the group and phase velocities exceed several hundred kilometers/sec, and these oscillations could propagate upstream to interact with incident particles (20).

Triggering of electrostatic plasma oscillations by charge separation electric fields has also been investigated, and these modes probably play a particularly significant role in producing particle acceleration by a stochastic Doppler-shifted mechanism (20, 21, 22). Indeed, even if plasma oscillations were not the waves which produced the primary acceleration, it has been shown (23) that the background plasma oscillation fields associated with a non-Maxwellian spectrum such as that of Fig. 1 are very large. Hence wave-particle interactions and electrostatic wave energy transport cannot be neglected. The electron plasma oscillation branch is of particular interest because these fast waves can also travel upstream to disturb incident plasma.

The results available to date suggest that charge-separation electric fields, high frequency wave modes, plasma instabilities, upstream propagation, non-linear wave-particle interactions, etc. are all important in the transition region, and these considerations would tend to explain why many detailed predictions of the fluid models are not verified by probes which examine microscopic phenomena. On the other hand, the gross agreement between the fluid predictions and the statistical location and shape of the magnetopause and shock boundary is probably simply explained by kinematic considerations; very crudely, the largest amplitude excitations induced in the wind will be those with wavelengths comparable to the scale size of the magnetosphere. Since these long wavelength oscillations (Alfvén or magnetosonic) are well described by the fluid equations, the fluid model can yield a meaningful set of statistical or average boundaries.

ACKNOWLEDGMENT

This work was supported in part by the National Aeronautics and Space Administration under Contract NASW-1366.

FIGURE CAPTIONS

Figure 1. Simultaneous interplanetary and transition region positive ion distributions (14).

Figure 2. Typical search coil magnetic power spectra (18).

REFERENCES

1. W. I. Axford, J.G.R., 67, 3791, 1962.
2. P. J. Kellogg, J.G.R., 67, 3805, 1962.
3. J. R. Spreiter and W. P. Jones, J.G.R., 68, 3555, 1963.
4. J. H. Wolfe, R. W. Silva, and M. A. Meyers, J.G.R., 71, 1319, 1965.
5. L. Lees, AIAA Journal, 2, 1576, 1964.
6. G. K. Walters, J.G.R., 69, 1769, 1964.
7. J. R. Spreiter, et al., Plan. Space Sci., 14, 223, 1966.
8. F. deHoffman and E. Teller, Phys. Rev., 80, 692, 1950.
9. J. W. Freeman, Jr., J. A. Van Allen and L. J. Cahill, Jr., J.G.R., 68, 2121, 1963.
10. J. W. Freeman, Jr., J.G.R., 69, 1691, 1964.
11. S. J. Bame, et a., Trans. A.G.U., 46, 142, 1965.
12. K. A. Anderson, H. K. Harris, and R. J. Paoli, J.G.R., 70, 1039, 1965.
13. C. Y. Fan, G. Gloeckler, and J. A. Simpson, J.G.R., 71, 1837, 1966.
14. J. H. Wolfe, R. W. Silva, and M. A. Meyers, Space Research VI, in press.
15. J. H. Wolfe, et al., J.G.R., 71, 3329, 1966.
16. F. L. Scarf, J. H. Wolfe, and R. W. Silva, to be published.
17. E. W. Greenstadt, et al., Trans. A.G.U., 47, 143, 1966.
18. R. E. Holzer, et al., J.G.R., 71, 1481, 1966.
19. P. D. Noerdlinger, J.G.R., 69, 369, 1964.
20. F. L. Scarf, Raumfahrtforschung, in press.
21. F. L. Scarf, W. Bernstein, and R. W. Fredricks, J.G.R., 70, 9, 1965.
22. P. A. Sturrock, Phys. Rev., 141, 186, 1966.
23. A. Eviatar, J.G.R., 71, 2715, 1966.

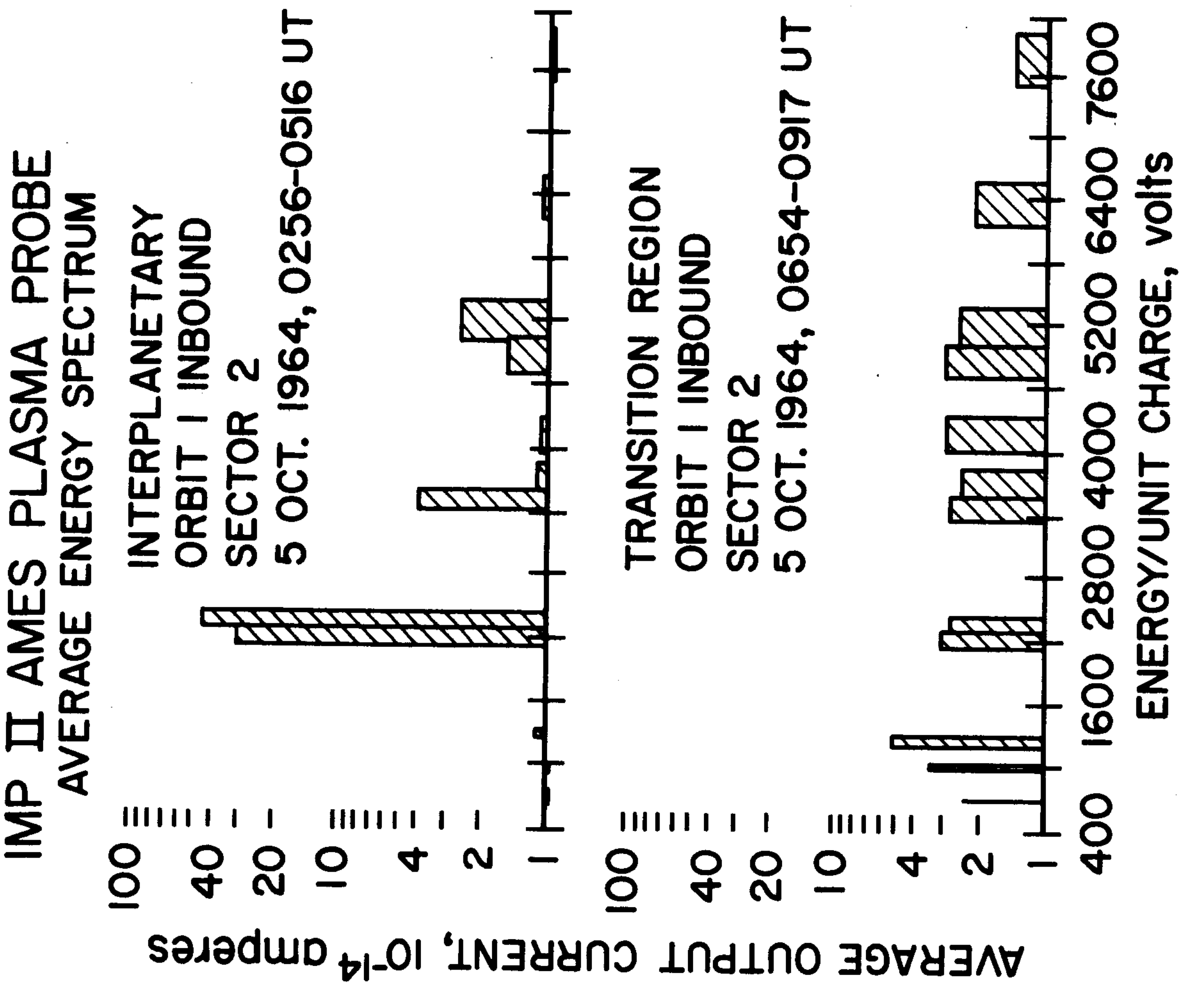
IMP II AMES PLASMA PROBE
AVERAGE ENERGY SPECTRUM
INTERPLANETARY
ORBIT I INBOUND
SECTOR 2
5 OCT. 1964, 0256-0516 UT
TRANSITION REGION
ORBIT I INBOUND
SECTOR 2
5 OCT. 1964, 0654-0917 UT
AVERAGE OUTPUT CURRENT, 10-14 amperes
100
40
20
10
4
2
1
400 1600 2800 4000 5200 6400 7600
ENERGY/UNIT CHARGE, volts

Figure 1

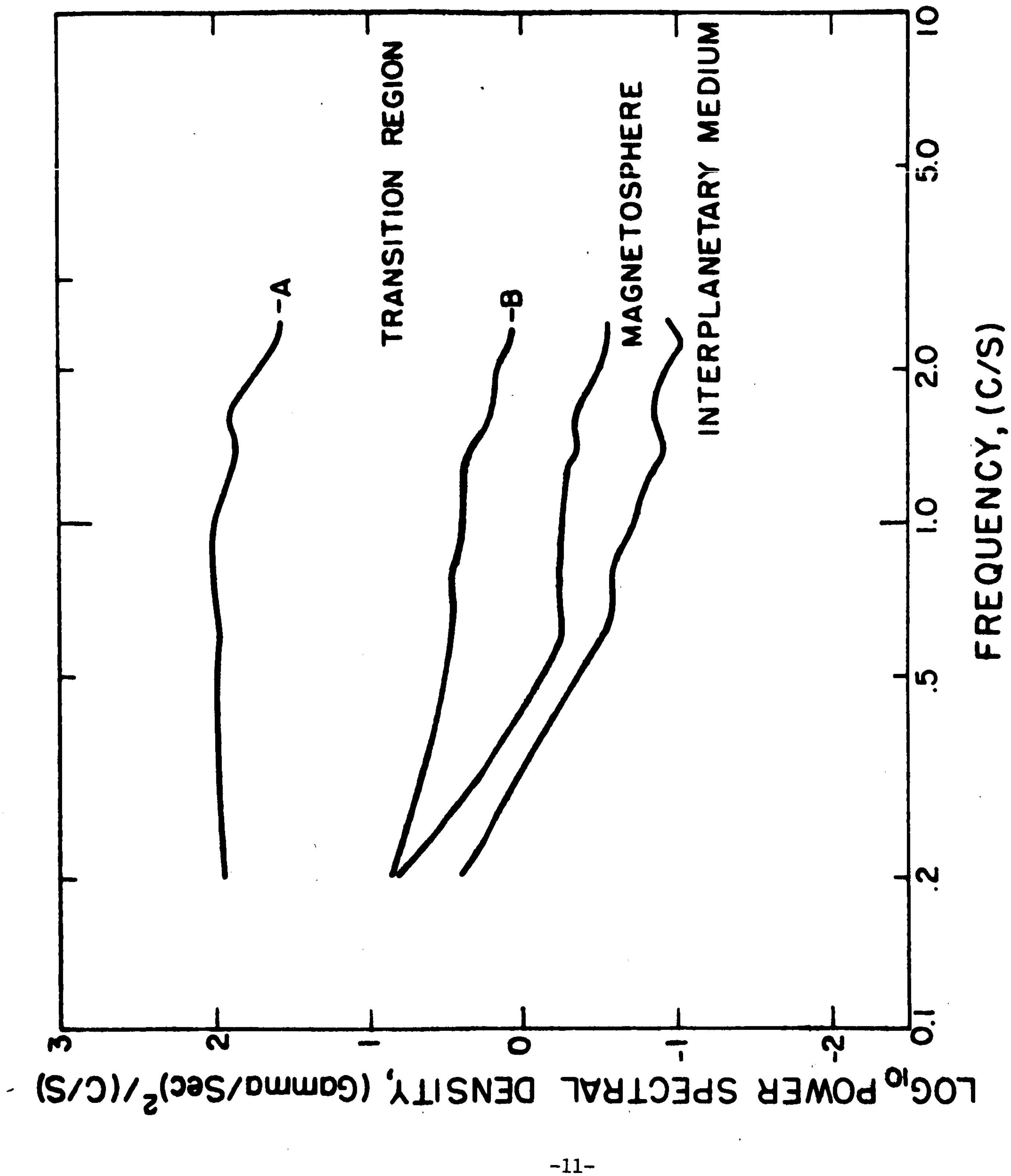
TRANSITION REGION
MAGNETOSPHERE
INTERPLANETARY MEDIUM
-A
-B
0.1
.2
.5
1.0
2.0
5.0
10
3
2
1
0
-1
-2
FREQUENCY, (C/S)
LOG$_{10}$ POWER SPECTRAL DENSITY, (Gamma/Sec)^2/(C/S)

Figure 2